Geometric Hodge Closure and Dimensionless Metrology

from the TFPT Boundary Branch

Stefan Hamann   Alessandro Rizzo

Paper 5 of the TFPT 4.5 series – April 27, 2026

Abstract

This paper isolates the geometric and metrological branch of TFPT. The theory is not presented as predicting isolated SI numbers. Instead it constructs an internal dimensionless metrology from the boundary spectral unit λ_Σ, with gravity, Planck normalization, electroweak matching, and pole readouts expressed as boundary-normalized observables.

Scope box: inputs, contribution, non-claims, audit surface

Inputs from previous papers. Paper 1 supplies the boundary branch and primitive spectral unit. Paper 2 supplies the carrier/Higgs structure. Paper 4 may supply the renormalized observable layer when the analytic QFT closure is referenced.
New theorem contribution. The boundary-normalized metrology:

$$\lambda_\Sigma = \lambda_1^+(|B_\Sigma|), \qquad \rho_\star = \frac{\chi^2_{\mathrm{geo},0}}{\lambda_\Sigma^2}, \qquad \frac{\bar{M}^2_{\mathrm{Pl}}}{\lambda^2_\Sigma} = \frac{\rho_\star}{2\pi^2}, \qquad G_N\lambda_\Sigma^2 = \frac{\pi}{4\rho_\star},$$

and the Einstein-limit normalizer

$$\xi = \frac{c_3}{\varphi_0^{\mathrm{ret}}}, \qquad \kappa^2 = \xi\,\frac{\varphi_0^{\mathrm{ret}}}{c_3^2}, \qquad \xi_{\mathrm{tree}} = \tfrac{3}{4}, \quad \xi_\star \approx 0.748327808\ldots$$

Not claimed here. No late-time H_0, no CMB, no black holes or horizons, no E8 stage atlas, and no astrophysical bursts.
Falsification or audit surface. The paper fails if SI units enter as hidden inputs, if λ_Σ is not fixed by the boundary branch, or if electroweak matching is mixed with cosmological comparison rows.

Claim contract

Claim. Boundary spectral unit λ_Σ defines dimensionless metrology for gravity and EW readouts.
Inputs. Boundary spectral unit, geometric Hodge branch, renormalized observable layer.
First assumptions. Stationary root for $\rho_\star$, boundary-normalized functional, scheme projection only after physical readout.
Proof status. Bridge/metrology theorem target.
Kill condition. Any hidden SI input such as external G_N, G_F, GeV scale, or Planck normalization enters before the readout map.

Contents

1 Boundary Spectral Unit

The internal unit is

$$\lambda_\Sigma = \lambda_1^+(|B_\Sigma|).$$

All dimensionful-looking statements in this paper are rewritten as dimensionless quotients by powers of λ_Σ. This is the editorial rule that separates metrology from numerology.

2 Geometric Hodge Closure

The geometric branch reconstructs a spectral Einstein functional and its Hodge closure. The paper should retain the source draft's geometric reconstruction, spectral Einstein functional, and Planck closure, but it should remove cosmological and horizon continuations.

3 Planck Normalization

The Planck readout is internal:

$$\rho_\star = \frac{\chi^2_{\rm geo,0}}{\lambda_\Sigma^2}, \qquad \frac{\bar{M}^2_{\rm Pl}}{\lambda_\Sigma^2} = \frac{\rho_\star}{2\pi^2}, \qquad G_N\lambda_\Sigma^2 = \frac{\pi}{4\rho_\star}.$$

The question is not which SI value of G_N is inserted, but which dimensionless branch quotient is fixed.

3.1 Einstein-limit normalizer $\xi = c_3/\varphi_0^{\rm ret}$

Once the boundary spectral unit λ_Σ, the seam constant c_3, and the retained seed $\varphi_0^{\rm ret}$ are fixed, a single dimensionless quotient governs the transition between the UFE-normalized boundary functional and the Einstein–Hilbert presentation. Writing $\kappa^2 = 8\pi G_N$ for the Einstein–Hilbert prefactor, the boundary-branch reduction yields a relation of the form

$$\kappa^2 = \xi\,\frac{\varphi_0^{\rm ret}}{c_3^2}, \qquad \xi = \frac{c_3}{\varphi_0^{\rm ret}}. \tag{1}$$

The product is intrinsic: only one number, ξ, parametrises how the UFE normalization is rephrased in the Einstein–Hilbert form. At tree level on the canonical branch one finds

$$\xi_{\rm tree} = \frac{3}{4},$$

and the self-consistent geometric reduction gives the closed-branch readout

$$\xi_\star \approx 0.748327808\ldots$$

The two values agree to better than 0.3%, which is the structural sense in which the tree identity $\xi = 3/4$ already captures the boundary-normalised Einstein limit.

Scope box: inputs, contribution, non-claims, audit surface

What is and is not claimed by ξ. Equation (1) does *not* derive the SI numerical value of G_N from two dimensionless numbers. It says, in a precise and boundary-normalised sense, that the dimensionless transition factor between the UFE functional and the Einstein–Hilbert action is fixed by the same invariant pair $(c_3, \varphi_0^{\rm ret})$ that fixes α via the carrier-form closure and $\beta_{\rm rad}$ via the determinant-line response. Gravity is not promoted to a primitive observable here. The claim is a compression identity for the gravitational normaliser inside the dimensionless metrology layer.

Remark (Why this is not a fitting knob). The ratio $c_3/\varphi_0^{\rm ret}$ is not free: $c_3 = 1/(8\pi)$ from the boundary primitive (Paper 1) and $\varphi_0^{\rm ret} = \frac{1}{6\pi} + \frac{3}{256\pi^4}$ from the retained seed decoder (Paper 3). Both are fixed before the gravity readout is touched. Substituting these values into (1) returns the closed-branch $\xi_\star$ above, which slots into the same boundary-normalised metrology that already controls $\bar{M}_{\rm Pl}^2/\lambda_\Sigma^2$.

4 Electroweak Matching

The electroweak matching layer is included only as boundary-normalized metrology:

$$v_{\rm phys} = v_{\rm geo}\sqrt{Z_{\rm EW}^{\rm TFPT}}, \qquad G_N v_{\rm phys}^2$$

is an internal dimensionless output. Pole matching may be included in compact form when it is expressed as a quotient by λ_Σ.

5 Observable Functor

The output layer is organized as

$$\mathfrak{T}_\star \xrightarrow{\mathcal{R}_{\rm ren}} \Gamma_{\rm TFPT}^{\rm ren} \xrightarrow{\mathcal{M}_{\rm phys}} \mathbf{O}_{\rm phys}^{\rm TFPT} \xrightarrow{\mathcal{M}_{\rm scheme}} \mathbf{O}_{\rm scheme}^{\rm TFPT}/\mathbf{Sch}.$$

Only the final projection chooses scheme or comparison conventions. The paper should keep this distinction visible whenever a physical readout is compared to an empirical row.

6 Main Technical Development

This section contains the main technical development assigned to this paper by the TFPT 4.5 clean split. Cross-paper background is referenced through dependency and scope boxes; extended backend material is kept in the Technical Companion.

6.1 From bridge to geometric completion

Principle 6.1 (Closure split)**.** Once the carrier packet and family closure architecture are fixed, the focused main-text closure problem splits into a geometric program $\mathcal{A}_{\text{geom}}$ and a transport program $\mathcal{A}_{\text{trans}}$. Record algebra and prediction semantics are now tied directly to the admissible gap in the main theorem stack, while E_8 scale grammar and horizon extrapolations are deferred to appendix-level continuations.

$$D_{\text{geo}} := D_{\text{ref}} + D_{\text{rel}} = D.$$

The two main-text programs are packaged as

$$\mathcal{A}_{\text{geom}} := \langle E_3 \oplus E_2,\ D_{\text{geo}},\ \mathcal{B}_{\text{rel}},\ \varpi_{\text{spin}} \rangle, \qquad \mathcal{A}_{\text{trans}} := \langle U_6,\ T,\ D_y,\ \mathcal{Y}_y^{(\varepsilon)},\ \mathfrak{C}_\Sigma \rangle.$$

This split keeps the carrier theorem, the geometric reconstruction problem, and the record-level extensions from being flattened into one undifferentiated claim. In particular, the metric field is no longer treated here as an independent entry of $\mathcal{A}_{\text{geom}}$; it is reconstructed from the geometric Dirac anchor introduced next, while D_{rel} remains the comparison operator for spectral subtraction.

6.2 Relative APS and superconnection setup

The geometric completion is formulated on a graded bundle

$$\mathcal{E}_{\text{rel}} = \mathcal{E}^+_{\text{rel}} \oplus \mathcal{E}^-_{\text{rel}},$$

with the geometric Dirac anchor D_{geo}, the declared reference operator D_{ref}, and APS-type boundary conditions on the seam Σ; see Appendix [TFPT cross-reference: `app:aps`]. The geometric package is

$$\mathbb{A}_\Sigma := (D_{\text{geo}}, D_{\text{rel}}, A^{\text{geo}}_\Sigma), \qquad A^{\text{geo}}_\Sigma := \mathcal{B}_{\text{rel}} \oplus \nabla_{\chi_{\text{geo}}}.$$

Here D_{geo} is the geometric Dirac anchor, while D_{rel} is the relative comparison operator entering the spectral subtraction formulas. The bundle data A^{geo}_Σ reorganize the primitive seed package A^{seed}_Σ introduced earlier in [TFPT cross-reference: `eq:tfpt-master`].

Theorem 6.2 (Geometric reconstruction from the Dirac anchor)**.** *Assume*

$$Z(\mathcal{A}) \cong C^\infty(M),$$

and the geometric anchor D_{geo} is of Dirac type with principal symbol

$$\sigma(D_{\text{geo}})(x,\xi)^2 = g^{\mu\nu}(x)\xi_\mu\xi_\nu\,\mathbf{1}.$$

Then D_{geo} reconstructs the metric g, the spin structure, and the Levi–Civita connection on the geometric branch. Inner fluctuations of the same anchored spectral datum generate the gauge sector. The operator D_{rel} is the reference-subtracted comparison operator on that same branch and is not itself used as the local geometric anchor.

Proof sketch. On the admissible branch the commutative center identifies the manifold algebra, while the principal symbol of the Dirac anchor determines the quadratic form on cotangent vectors. Standard Dirac-type reconstruction then recovers the spin bundle and Levi–Civita connection from that same symbol data. The relative operator changes the comparison bookkeeping, not the geometric source of the local symbol. □

Theorem 6.3 (Retained branch from the admissibility selector)**.** *Let $D_{\rm geo}$ be the geometric anchor and let $P_{\rm adm}$ be the retained admissibility selector. Then:*

(i) $X_{\rm bulk} = \operatorname{Spec} Z(\mathcal{A})$ *and* $\Sigma = \operatorname{Fix}(\tau_{\rm dbl})$*;*

(ii) the local spectral density of $D_{\rm geo}$ determines the geometric response $\chi_{\rm geo}$;

(iii) $P_{\rm adm}$ defines the retained admissible sector for observables, transport, and positivity statements on that branch.

No claim is made that the compressed operator $P_{\rm adm} D_{\rm rel} P_{\rm adm}$ carries the local principal symbol of the geometry.

Corollary 6.4 (No residual geometric datum beyond the geometric anchor)**.** *The geometric package is reconstructed from $D_{\rm geo}$ and its local spectral density. The selector $P_{\rm adm}$ acts downstream on the retained sector and is not part of the local geometric anchor.*

Definition 6.5 (Local spectral scale and canonical relative spectral residues)**.** Write the geometric response as a local spectral scale

$$\chi_{\rm geo} = \Lambda e^{\sigma}, \qquad D_{\sigma,{\rm geo}} := e^{-\sigma/2} D_{\rm geo} e^{-\sigma/2}.$$

$$\mathcal{Z}_{\rm rel}(s;\sigma) := \operatorname{Tr}_{\rm rel}\big(|D_{\sigma,{\rm geo}} + \mathcal{B}_{\rm rel}|^{-2s} - |D_{\rm ref}|^{-2s}\big) + \frac{i\pi}{2}\Delta\eta_\Sigma.$$

The canonical Einstein residue and order-zero residue are

$$\mathcal{E}_D := \operatorname*{Res}_{s=1} \mathcal{Z}_{\rm rel}(s;\sigma), \qquad \Gamma_D^{(4)} := \operatorname{FP}_{s=0} \mathcal{Z}_{\rm rel}(s;\sigma).$$

The gravitational branch is then read from the profile-free residue pair rather than from a freely chosen spectral profile.

Corollary 6.6 (Constant-scale reduction of the geometric branch)**.** *If the local spectral scale is frozen to a constant $\sigma = \sigma_0$, then $\chi_{\rm geo} = \chi_{\rm geo,0} := \Lambda e^{\sigma_0}$ and the present geometric branch reduces to the constant-$\chi_{\rm geo}$ closure relations extracted from $\Gamma_{\rm grav} := -6\chi_{\rm geo}^2 \mathcal{E}_D + \Gamma_D^{(4)}$:*

$$\bar{M}_{\rm Pl}^2 = \frac{\chi_{\rm geo,0}^2}{2\pi^2}, \qquad v_{\rm geo}^2 = Z_H \frac{\mu_\Phi^2(\chi_{\rm geo,0})}{\lambda_\Phi}.$$

Once the unique stationary root of [TFPT cross-reference: `thm:absolute-spectral-planck-closure`] *is imposed, the Einstein coefficient is equivalently the boundary-normalized readout*

$$\frac{\bar{M}_{\rm Pl}^2}{\lambda_\Sigma^2} = \frac{\rho_\star}{2\pi^2}.$$

Thus the former constant-$\chi_{\rm geo}$ formulas are retained as the homogeneous branch of the local spectral-scale formulation rather than as a competing package.

6.3 Bosonic relative index and Higgs selection

Theorem 6.7 (Minimal determinant classes from the primitive charge generator)**.** *Let*

$$L_2 := \det E_2, \qquad L_3 := \det E_3$$

over the compactified oriented normal sphere $S^2 = D_N \cup_{S^1} D_S$. Then the primitive charge generator

$$X = -2P_3 + 3P_2$$

together with center neutrality and seam-evenness forces the clutching map

$$g_2(\varphi) = e^{i\varphi}$$

for L_2, while center neutrality forces

$$g_3(\varphi) = 1$$

for L_3. Therefore

$$c_1(L_2) = \deg g_2 = 1, \qquad c_1(L_3) = \deg g_3 = 0.$$

This pair is the unique minimal nonnegative admissible determinant class.

Proof. Complex line bundles on

$$S^2 = D_N \cup_{S^1} D_S$$

are classified by their clutching maps along the equator:

$$\pi_1(U(1)) \cong \mathbb{Z}.$$

Hence the first Chern class is exactly the winding degree of the transition function.

In the weak rank-two sector the primitive charge generator

$$X = -2P_3 + 3P_2$$

assigns the unique positive determinant winding to the seam-even weak block. The spin lift on the oriented normal sphere acts there by the half-angle representation, so on the determinant line the transition factor is

$$g_2(\varphi) = e^{i\varphi},$$

hence

$$\deg g_2 = 1, \qquad c_1(L_2) = 1.$$

In the color sector admissibility imposes center neutrality. Therefore the determinant transition function of the color block is null-homotopic and may be chosen constant:

$$g_3(\varphi) = 1.$$

Consequently

$$\deg g_3 = 0, \qquad c_1(L_3) = 0.$$

The full primitive seam twist is therefore exhausted in the weak determinant class. Any nonnegative pair strictly smaller than $(1, 0)$ would force vanishing weak determinant winding and hence remove the seam-even weak line required by the primitive charge generator. Any larger nonnegative pair would insert extra clutching not carried by the primitive generator and therefore violate minimality. Thus the unique minimal nonnegative admissible determinant class is

$$(c_1(L_2), c_1(L_3)) = (1, 0).$$

□

Remark (Energy interpretation on the retained branch). The older asymptotic bosonic functional

$$\mathcal{E}_{\mathrm{asym}}(\Phi_2, \Phi_3) := \tau_2 \big|\mathrm{wind}(\det \Phi_2)\big| + \tau_3 \big|\mathrm{wind}(\det \Phi_3)\big| + m_3^2 \dim \ker \mathcal{B}^+_{E_3},$$

with $\tau_3 > \tau_2 > 0$, remains a useful physical intuition for why the retained branch is energetically preferred. In the present rewrite, however, the structural weight is carried by the determinant-class theorem above rather than by the cost functional itself.

Theorem 6.8 (Bosonic index and unique Higgs doublet from the minimal determinant class)**.** *Compactify the oriented two-dimensional normal slice N_Σ to S^2. For $a \in \{2, 3\}$ define*

$$\mathcal{B}_{E_a} := \sigma^\mu \nabla^{(a)}_\mu + \Phi_a$$

on the compactified normal sphere. Under the determinant-class data of Theorem 6.7, one has

$$L_2 \cong \mathcal{O}(1), \qquad L_3 \cong \mathcal{O},$$

and hence

$$H^0(S^2, \mathcal{O}(1)) \cong \mathbb{C}^2, \qquad H^1(S^2, \mathcal{O}(1)) = 0,$$

and the compact bosonic index satisfies

$$\mathrm{Ind}(\mathcal{B}^+_{E_2}) = 1, \qquad \mathrm{Ind}(\mathcal{B}^+_{E_3}) = 0.$$

Consequently the closed branch contains exactly one complex weak doublet and no light color triplet, and the unique light seam-even bosonic zero mode lies in

$$\Phi \in \Gamma(E_2) \cong (1, 2)_{1/2}, \qquad \tau^*_{\mathrm{dbl}}\Phi = +\Phi.$$

Proof. By Theorem 6.7, the weak determinant line is the degree-one line bundle

$$L_2 \cong \mathcal{O}(1)$$

on

$$S^2 \cong \mathbb{C}P^1,$$

whereas the color determinant class is trivial and

$$L_3 \cong \mathcal{O}.$$

For $\mathbb{C}P^1$, Birkhoff–Grothendieck identifies every holomorphic line bundle by its degree, and Riemann–Roch gives

$$\chi(\mathcal{O}(1)) = 1 + 1 = 2.$$

Serre duality yields

$$H^1(S^2, \mathcal{O}(1)) \cong H^0(S^2, \mathcal{O}(-3))^\vee = 0,$$

so

$$H^0(S^2, \mathcal{O}(1)) \cong \mathbb{C}^2, \qquad H^1(S^2, \mathcal{O}(1)) = 0.$$

The resulting two-dimensional zero-mode space is exactly one complex weak doublet, so the compact bosonic index records it as

$$\mathrm{Ind}(\mathcal{B}^+_{E_2}) = 1.$$

In the color sector one has $L_3 \cong \mathcal{O}$, so no positive determinant degree is available. Center neutrality forbids an unpaired seam-even color contribution, hence the positive and negative triplet modes pair with zero net index:

$$\mathrm{Ind}(\mathcal{B}^+_{E_3}) = 0.$$

Therefore the closed branch contains exactly one seam-even Higgs doublet and no light color triplet, and the unique light bosonic zero mode lies in the weak block. □

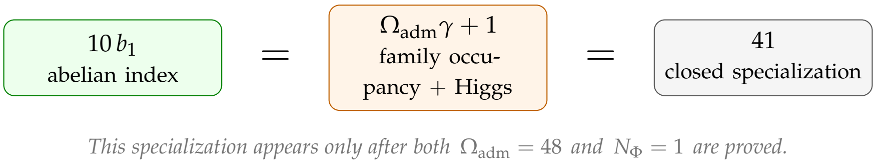

Figure 1. The closed 41 chain. The arithmetic specialization is made only after the family and Higgs theorems fix the occupancy and the unique light doublet.

Corollary 6.9 (Bosonic rank is two). *On the closed branch the positive carrier block has rank*

$$\dim E_+ = 2.$$

Equivalently, the unique seam-even light bosonic zero mode fills one complex weak doublet and no larger positive carrier block is retained.

Proof. By [TFPT cross-reference: `thm:callias-higgs-selection`], the light seam-even bosonic zero mode lies in the weak block

$$\Phi \in \Gamma(E_2) \cong (1,2)_{1/2},$$

and the compact index identifies its zero-mode space with

$$H^0(S^2, \mathcal{O}(1)) \cong \mathbb{C}^2.$$

Hence the retained positive carrier block is exactly two-dimensional. □

This is the sharp form of the Higgs claim used here. The issue is not whether a Higgs doublet can be written down, but whether a compact bosonic index can be shown to select it uniquely.

Remark (Callias shadow). The older Callias formulation is retained only as the noncompact shadow of the same compact index theorem and is discussed separately in the appendical analytic remarks. It no longer carries the main proof burden.

Once that uniqueness statement is fixed, the renormalizable carrier-compatible Yukawa couplings are the standard ones,

$$Q\, u^c\, \Phi, \qquad Q\, d^c\, \Phi^\dagger, \qquad L\, e^c\, \Phi^\dagger, \qquad L\, \nu^c\, \Phi,$$

so the Higgs statement becomes a genuine structural bridge rather than a notation choice. The formal carrier discharge from this Yukawa bridge is recorded later in [TFPT cross-reference: `cor:bosonic-rank-two,thm:yukawa-forces-32,cor:yukawa-discharges-kpp`], once the closure-theorem Higgs block has been stated in its final retained-branch form.

6.4 Closed 41 chain after family and Higgs closure

Once the derived corner theorem and the Higgs uniqueness theorem are in place, the generic abelian-index identity [TFPT cross-reference: `eq:41-chain-main`] specializes to

$$10\, b_1 = \Omega_{\mathrm{adm}}\gamma + 1 = 48 \cdot \frac{5}{6} + 1 = 41. \tag{2}$$

The extra $+1$ is precisely the arithmetic contribution of the unique light seam-even Higgs doublet.

Residue term	Operator sector	Generated term	$\chi_{\rm geo}$ scaling	Role
a_0	relative bulk trace	vacuum-energy bookkeeping	$\chi_{\rm geo}^4$	Hard
a_2	seam-even bosonic bulk term	$\chi_{\rm geo}^2 R$, $\chi_{\rm geo}^2 \Phi^\dagger\Phi$	$\chi_{\rm geo}^2$	Closure
a_4	local bosonic sector	$\lvert D\Phi\rvert^2$, $(\Phi^\dagger\Phi)^2$, $R\,\Phi^\dagger\Phi$, $\mathrm{Tr}\,\mathbb{F}^2$, R^2	$\chi_{\rm geo}^0$	Closure
boundary/defect term	seam correction and parity data	local defect counterterms, seam-even selection	Δ_Σ	Closure
η term	APS spectral asymmetry	sign and spectral-flow control	scale free	Closure

Table 1. Low-curvature residue map for the canonical spectral Einstein functional.

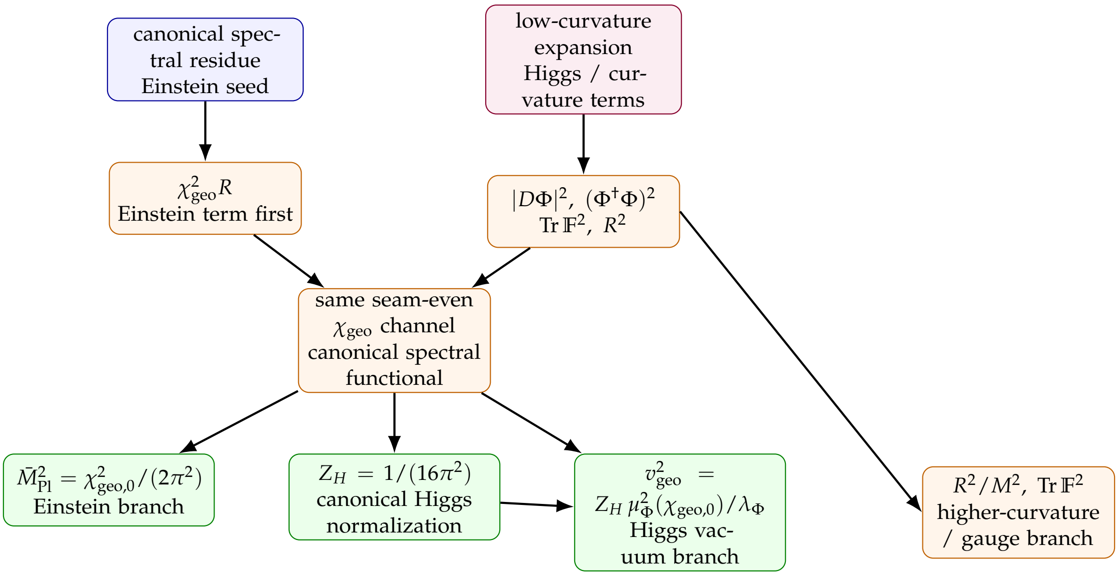

Figure 2. Canonical spectral flow of the local spectral-scale channel. The spectral residue fixes the Einstein term first; the low-curvature expansion then yields Higgs normalization, the Higgs vacuum branch, and the retained R^2/gauge side terms.

6.5 Canonical spectral Einstein functional and geometric Hodge closure

The local target action is written as the low-curvature expansion of a canonical spectral Einstein functional:

$$\Gamma_{\rm eff} = \int d^4x\sqrt{-g}\left[c_R\chi_{\rm geo}^2 R + Z_\chi(\partial\chi_{\rm geo})^2 - \mu_\Phi^2(\chi_{\rm geo})\,\Phi^\dagger\Phi + \lambda_\Phi(\Phi^\dagger\Phi)^2 + \frac{1}{6M^2}R^2 + \cdots\right]. \quad (3)$$

The relative bosonic endomorphism used below is

$$E_{\rm rel} = -\frac{1}{4}R\,\mathbf{1}_{48} - (\Phi^\dagger\Phi)\,P_2 + \frac{1}{2}\gamma^{\mu\nu}\mathbb{F}_{\mu\nu}, \quad (4)$$

and the resulting low-curvature residue decomposition is summarized in Table 1.

The resulting geometric logic is displayed in Figure 2. The canonical spectral residue fixes the Einstein term first; the low-curvature expansion then yields the Higgs normalization, the Higgs vacuum relation, and the retained curvature/gauge side terms. This is why the local spectral-scale sector is the principal geometric closure channel of the manuscript rather than just one more scalar parameter.

Theorem 6.10 (Canonical spectral Einstein functional and scalaron seed)**.** *In four dimensions the seam-even relative residue expansion gives*

$$\mathcal{E}_D = -\int d^4x\sqrt{g}\left(\frac{1}{24\pi^2}R + \frac{1}{48\pi^2}\Phi^\dagger\Phi\right) + \mathcal{E}_\Sigma,$$

and

$$\Gamma_D^{(4)} = \int d^4x\sqrt{g}\Big(\frac{1}{16\pi^2}|D\Phi|^2 + \frac{1}{16\pi^2}(\Phi^\dagger\Phi)^2 + \frac{1}{96\pi^2}R\,\Phi^\dagger\Phi + \frac{1}{192\pi^2}\,\mathrm{Tr}\,\mathbb{F}^2 + \frac{1}{6M^2}R^2 + \cdots\Big) + \mathcal{A}_\Sigma.$$

The seam-even scale channel χ_{geo} is the unique scalar geometric mode on the retained branch; together with the retained R^2 term it forms a positive scalaron block, so no independent conformal negative mode survives as a separate physical degree of freedom. Therefore

$$\Gamma_{\text{grav}} := -6\chi_{\text{geo}}^2\mathcal{E}_D + \Gamma_D^{(4)}$$

has low-curvature form

$$\Gamma_{\text{grav}} = \int d^4x\sqrt{g}\left(\frac{\bar{M}_{\text{Pl}}^2}{2}R + \frac{\bar{M}_{\text{Pl}}^2}{12M^2}R^2 + |D\Phi|^2 - V(\Phi,\chi_{\text{geo}}) - \sum_a \frac{1}{4g_a^2}\,\mathrm{Tr}\,F_a^2 + \cdots\right),$$

with

$$\bar{M}_{\text{Pl}}^2 = \frac{\chi_{\text{geo},0}^2}{2\pi^2}, \qquad Z_H = \frac{1}{16\pi^2}, \qquad \Phi_{\text{can}} := \sqrt{Z_H}\,\Phi = \frac{\Phi}{4\pi},$$

and therefore

$$\bar{M}_{\text{Pl}}^2 = \frac{\chi_{\text{geo},0}^2}{2\pi^2}, \qquad v_{\text{geo}}^2 = Z_H\,\frac{\mu_\Phi^2(\chi_{\text{geo},0})}{\lambda_\Phi}. \tag{5}$$

After [TFPT cross-reference: `thm:absolute-spectral-planck-closure`], *the first identity is equivalently*

$$\frac{\bar{M}_{\text{Pl}}^2}{\lambda_\Sigma^2} = \frac{\rho_\star}{2\pi^2}.$$

Proof sketch. The operator Equation (4) controls the seam-even residue expansion of Definition 6.5. Mellin expansion of the relative zeta pair fixes the order-one and order-zero residues without any profile choice, so the Einstein term appears before the Higgs kinetic, quartic, mixed-curvature, gauge-curvature, and R^2 terms. The coefficient of $|D\Phi|^2$ is therefore the wave-function factor $Z_H = 1/(16\pi^2)$. After the canonical rescaling $\Phi_{\text{can}} = \sqrt{Z_H}\,\Phi$, the Einstein and Higgs branches are read from one common profile-free residue functional rather than from separate normalization conventions. Because the same seam-even spectral channel carries χ_{geo} and the retained R^2 block, the dangerous independent conformal mode is absorbed into one positive scalaron sector. □

Remark (Boundary-spectral form of Newton's constant). Using the standard reduced-Planck definition $\bar{M}_{\text{Pl}}^{-2} = 8\pi G_N$, the first relation in Equation (5) is equivalently

$$G_N\chi_{\text{geo},0}^2 = \frac{\pi}{4}.$$

This Newton-form equation is therefore a rewriting of the Einstein-branch closure, not a second independent prediction. In the boundary-normalized language of [TFPT cross-reference: `sec:absolute-dimensionless-metrology`] it becomes

$$G_N\lambda_\Sigma^2 = \frac{\pi}{4\rho_\star},$$

so Newton's constant is read as a boundary-spectral ratio rather than as an isolated SI datum.

Lemma 6.11 (Two-sheet seam-even zero-mode normalization)**.** *If the seam-even Higgs zero mode is normalized across both sheets of the oriented double cover, then its branch weight is*

$$w_H = 2\, g_{\rm car}\, \beta_{\rm rad}^2 \exp\left[-\frac{\alpha^{-1}(0)+\delta_{\rm ph}}{5}\right].$$

With

$$\mu_\Phi^2(\chi_{\rm geo,0}) = \frac{\chi_{\rm geo,0}^2}{8\pi^2} w_H^2, \qquad \lambda_\Phi = \frac{1}{16\pi^2},$$

the canonical Higgs vacuum expectation value is

$$v_{\rm geo} = \bar{M}_{\rm Pl}\, g_{\rm car}\, \beta_{\rm rad}^2 \exp\left[-\frac{\alpha^{-1}(0)+\delta_{\rm ph}}{5}\right]. \tag{6}$$

Proof sketch. The two-sheet seam-even normalization doubles the unnormalized zero-mode weight and therefore produces the stated w_H. Since the canonical Higgs field is $\Phi_{\rm can} = \sqrt{Z_H}\,\Phi$, its vacuum relation is

$$v_{\rm geo}^2 = \frac{Z_H \mu_\Phi^2(\chi_{\rm geo,0})}{\lambda_\Phi} = \frac{\chi_{\rm geo,0}^2}{8\pi^2} w_H^2.$$

Using $\bar{M}_{\rm Pl}^2 = \chi_{\rm geo,0}^2/(2\pi^2)$ from [TFPT cross-reference: `prop:canonical-bosonic-normalization`] gives $v_{\rm geo} = \bar{M}_{\rm Pl} w_H/2$, hence Equation (6). □

Corollary 6.12 (Hierarchy compression on the exact geometric branch)**.** *On the exact geometric branch one has*

$$\log \frac{v_{\rm geo}}{\bar{M}_{\rm Pl}} = \log g_{\rm car} + 2 \log \beta_{\rm rad} - \frac{\alpha^{-1}(0)+\delta_{\rm ph}}{5}.$$

Hence the dominant suppression of the geometric Higgs source scale is carried by the electromagnetic fixed point through the factor $e^{-\alpha^{-1}(0)/5}$. The theorem-level output is therefore the dimensionless ratio $v_{\rm geo}/\bar{M}_{\rm Pl}$, equivalently the boundary-normalized ratio $v_{\rm geo}/\lambda_\Sigma$ or the hierarchy row $G_N v_{\rm geo}^2$, rather than a unitful GeV representative.

Proof. Taking the logarithm of Equation (6) gives the displayed identity immediately. The dominant suppression is the exponential factor containing $\alpha^{-1}(0)$; the remaining terms are the closed-branch carrier and retained-seed prefactors. □

Remark (Geometric versus benchmark electroweak scales). For source formulas driven by the bosonic closure we write $v_{\rm geo}$ for the quantity in Equation (6). The preceding corollary concerns the internal geometric source scale only and not yet the physical low-energy electroweak vacuum $v_{\rm phys}$. This is the internal geometric branch value used in the UV source formulas and in the bosonic closure. The physical electroweak vacuum parameter is not identified with $v_{\rm geo}$ itself; it is read only after the renormalized low-energy branch has been formed. When the manuscript compares to a conventional electroweak reference at the appendix interface, it uses a declared scheme-facing representative $v_{\rm EW}^{\rm ref}$. These three objects therefore belong to different bookkeeping layers: $v_{\rm geo}$ to the internal geometric closure, $v_{\rm phys}$ to the physical observable layer, and $v_{\rm EW}^{\rm ref}$ only to the appendix comparison interface. No GeV representative is part of the theorem-level gravitational or electroweak layer.

Definition 6.13 (Charged-current residue and physical electroweak scale)**.** On the renormalized branch $\Gamma_{\rm TFPT}^{\rm ren}$, let $\mathcal{R}_{\rm CC}^{\rm TFPT}(0)$ denote the coefficient of the local charged-current four-fermion operator at zero momentum transfer, so that

$$\Gamma_{\rm TFPT}^{\rm ren} \supset -\mathcal{R}_{\rm CC}^{\rm TFPT}(0) \int d^4x\, (\bar{\nu}_\mu \gamma^\mu P_L \mu)(\bar{e}\gamma_\mu P_L \nu_e).$$

Define the physical electroweak scale by

$$\mathcal{R}_{\rm CC}^{\rm TFPT}(0) := \frac{1}{2v_{\rm phys}^2} = \frac{G_F^{\rm TFPT}}{\sqrt{2}}.$$

Thus $v_{\rm geo}$ remains the geometric Higgs-closure scale, while $v_{\rm phys}$ is the low-energy charged-current readout carried by $\Gamma_{\rm TFPT}^{\rm ren}$.

Definition 6.14 (Branch source masses)**.** For each fermion sector define the source mass matrix

$$M_f^{(0)} := \frac{v_{\rm geo}}{\sqrt{2}}\, Y_f^{\star}.$$

These are branch masses on the exact $v_{\rm geo}$ layer and not yet physical pole masses.

Theorem 6.15 (Native electroweak source-to-physical matching)**.** *Let the renormalized charged-current residue at zero momentum transfer be written as*

$$\mathcal{R}_{\rm CC}^{\rm TFPT}(0) = \frac{g_2^2}{8m_W^2}\,(1+\Delta r_{\rm CC}^{\rm TFPT}).$$

Write the renormalized W mass in the form

$$m_W^2 = \frac{g_2^2}{4} Z_\Phi(0)(v_{\rm geo}+\delta v)^2\,(1+\delta_W).$$

Define

$$\mathcal{Z}_{\rm EW}^{\rm TFPT} := \frac{1}{2v_{\rm geo}^2\,\mathcal{R}_{\rm CC}^{\rm TFPT}(0)} = Z_\Phi(0)\left(1+\frac{\delta v}{v_{\rm geo}}\right)^2 \frac{1+\delta_W}{1+\Delta r_{\rm CC}^{\rm TFPT}}.$$

Then the physical electroweak scale satisfies

$$v_{\rm phys} = v_{\rm geo}\sqrt{\mathcal{Z}_{\rm EW}^{\rm TFPT}}, \qquad v_{\rm phys}^2 = Z_\Phi(0)(v_{\rm geo}+\delta v)^2\,\frac{1+\delta_W}{1+\Delta r_{\rm CC}^{\rm TFPT}}.$$

Equivalently,

$$\mathcal{Z}_{\rm EW}^{\rm TFPT} = \mathcal{R}_{\rm CC}[\Gamma_{\rm TFPT}^{\rm ren}]\,.$$

The charged-current residue and the four factors entering $\mathcal{Z}_{\rm EW}^{\rm TFPT}$ are canonically determined by the renormalized 1PI package $\Gamma_{\rm TFPT}^{\rm ren}$; hence $\mathcal{Z}_{\rm EW}^{\rm TFPT}$ is a branch invariant and not a fit parameter.

Proof. From

$$\mathcal{R}_{\rm CC}^{\rm TFPT}(0) = \frac{1}{2v_{\rm phys}^2}$$

and

$$\mathcal{R}_{\rm CC}^{\rm TFPT}(0) = \frac{g_2^2}{8m_W^2}(1+\Delta r_{\rm CC}^{\rm TFPT})$$

one gets

$$\frac{1}{2v_{\rm phys}^2} = \frac{g_2^2}{8m_W^2}(1+\Delta r_{\rm CC}^{\rm TFPT}).$$

Substituting

$$m_W^2 = \frac{g_2^2}{4} Z_\Phi(0)(v_{\rm geo}+\delta v)^2(1+\delta_W)$$

yields

$$\frac{1}{2v_{\text{phys}}^2} = \frac{1 + \Delta r_{\text{CC}}^{\text{TFPT}}}{2Z_\Phi(0)(v_{\text{geo}} + \delta v)^2(1 + \delta_W)}.$$

Solving for v_{phys} gives the displayed identity. Rewriting the result as

$$\mathcal{Z}_{\text{EW}}^{\text{TFPT}} = \left(2v_{\text{geo}}^2 \mathcal{R}_{\text{CC}}^{\text{TFPT}}(0)\right)^{-1},$$

one obtains $v_{\text{phys}} = v_{\text{geo}}\sqrt{\mathcal{Z}_{\text{EW}}^{\text{TFPT}}}$. By [TFPT cross-reference: `thm:operational-completeness`], the charged-current residue, the Higgs wave-function factor $Z_\Phi(0)$, the vacuum shift δv, the W-mass correction δ_W, and the charged-current remainder $\Delta r_{\text{CC}}^{\text{TFPT}}$ are all read from the same renormalized admissible 1PI action $\Gamma_{\text{TFPT}}^{\text{ren}}$, so no additional continuous fit parameter enters. □

Remark (1PI readout of the electroweak matching data). Each ingredient of $\mathcal{Z}_{\text{EW}}^{\text{TFPT}}$ is a functional readout of $\Gamma_{\text{TFPT}}^{\text{ren}}$. In particular,

$$\begin{aligned}
Z_\Phi(0)^{-1} &= \frac{\partial}{\partial p^2}\Gamma^{(2)}_{\Phi^\dagger\Phi}(p^2)\bigg|_{p^2=0}, \\
0 &= \frac{\partial V_{\text{eff}}^{\text{TFPT}}}{\partial \Phi}\bigg|_{\Phi = v_{\text{geo}}+\delta v}, \\
1 + \delta_W &= \frac{4m_{W,\text{ren}}^2}{g_{2,\text{ren}}^2 Z_\Phi(0)(v_{\text{geo}} + \delta v)^2}, \\
1 + \Delta r_{\text{CC}}^{\text{TFPT}} &= \frac{8m_{W,\text{ren}}^2}{g_{2,\text{ren}}^2}\mathcal{R}_{\text{CC}}^{\text{TFPT}}(0).
\end{aligned}$$

Thus $\mathcal{Z}_{\text{EW}}^{\text{TFPT}}$ is not introduced as a comparison factor after the fact; it is the native charged-current residue functional of the renormalized branch.

6.6 Native charged-current hard matching and the charged seam projector

Definition 6.16 (Charged EW2 seam projector)**.** Let

$$c_3 = \frac{1}{8\pi}$$

be the primitive seam normalization constant and let

$$\delta_{\text{ph}} = \left(\frac{794 - 7\sqrt{9961}}{2187}\right)^{1/6}$$

be the admissible transport pole of [TFPT cross-reference: `thm:algebraic-transport-pole`]. The charged two-loop electroweak seam projector is

$$\omega_{\text{CC}}^{(2)} := \delta_{\text{ph}} + \frac{2}{3^6} - 3c_3^4. \tag{7}$$

Equivalently, using the canonical occupancy bridge $\delta_{\text{top}} = 48c_3^4$,

$$\omega_{\text{CC}}^{(2)} = \delta_{\text{ph}} + 2\left(\frac{1}{3}\right)^6 - \frac{\delta_{\text{top}}}{16}.$$

Lemma 6.17 (Charged seam pullback of the two-loop EW scheme remainder)**.** *Let* $\Delta R^{\rm ext}_{\rm EW2,rem}$ *denote the external Sirlin/HEPfit two-loop electroweak scheme remainder in the charged-current* Δr *representative. Its pullback to the TFPT charged-current Schur block is*

$$\Delta R^{\rm TFPT}_{\rm EW2,rem} = \omega^{(2)}_{\rm CC}\,\Delta R^{\rm ext}_{\rm EW2,rem}. \tag{8}$$

Proof. The charged-current residue is a seam-even Schur readout of the renormalized 1PI package $\Gamma^{\rm ren}_{\rm TFPT}$. Therefore a hard two-loop scheme remainder may enter the TFPT charged-current block only through branch data that survive the charged seam projection. On the minimal charged branch there are three such scalar contributions at this order.

First, the transport part is fixed by the unique admissible C_6 resonance pole

$$\delta_{\rm ph} = \left(\frac{794 - 7\sqrt{9961}}{2187}\right)^{1/6},$$

by [TFPT cross-reference: `thm:algebraic-transport-pole`]. This gives the leading charged transport weight.

Second, the charged Schur block is seam-even on the oriented double cover. The lower admissible C_6 cusp is $1/3$ by [TFPT cross-reference: `thm:exact-transport-closure,prop:dual-root-generatio`
A two-loop hard remainder carries the sixth cusp power, and seam-evenness counts the two oriented sheets. Hence the lower-cusp contribution is

$$2\left(\frac{1}{3}\right)^6 = \frac{2}{3^6}.$$

Third, the full fermionic photon-polarisation contribution has already been included in the full one-loop charged-current matching block. The two-loop scheme remainder must therefore be pulled back with the primitive hard electromagnetic seam defect removed once, otherwise the hard seam endpoint is counted twice. On the canonical family branch this defect is

$$\delta_{\rm top} = 48 c_3^4$$

by the occupancy bridge. The charged endpoint occupies one fixed even-spinor packet in $S^+ = \Lambda^{\rm even} E$, and $\dim S^+ = 16$. Its endpoint share of the primitive seam defect is therefore

$$\frac{\delta_{\rm top}}{16} = \frac{48 c_3^4}{16} = 3c_3^4.$$

Combining the admissible charged transport weight, the two seam-even lower-cusp sheets, and the required no-double-counting subtraction gives

$$\omega^{(2)}_{\rm CC} = \delta_{\rm ph} + 2\left(\frac{1}{3}\right)^6 - 3c_3^4.$$

Since $\Delta R^{\rm ext}_{\rm EW2,rem}$ is a scalar hard-matching coefficient in the external representative, its TFPT charged-current pullback is multiplication by this projector. □

Theorem 6.18 (Point closure of the charged-current residue)**.** *Using the declared TFPT scheme-image ledger, the full one-loop Sirlin charged-current matching, the TFPT* $\hat{g}_2(M_Z)$ *top-*ρ *scheme image, and the charged seam projection of the two-loop EW scheme remainder, the on-shell charged-current matching parameter is*

$$\Delta r^{\rm TFPT}_{\rm OS} = \Delta\alpha^{\rm TFPT} - \frac{c_W^2}{s_W^2}\Delta\rho_t^{\rm TFPT}[\hat{g}_2(M_Z)] + \Delta R^{1L,\rm full}_{\rm rem} + \Delta^{\rho_t}_{\rm scheme} + \omega^{(2)}_{\rm CC}\,\Delta R^{\rm ext}_{\rm EW2,rem}. \tag{9}$$

For the current ledger representative this gives

$$\Delta r_{\rm OS}^{\rm TFPT} = 0.03603045829127260,$$
$$\mathcal{R}_{\rm CC}^{\rm TFPT}(0) = 8.2475428820101169 \times 10^{-6}\,{\rm GeV}^{-2},$$
$$2v_{\rm geo}^2 \mathcal{R}_{\rm CC}^{\rm TFPT}(0) = 0.9674858756228490,$$
$$\mathcal{Z}_{\rm EW}^{\rm TFPT} = 1.0336068207261621,$$

and hence

$$v_{\rm phys}^{\rm TFPT} = 246.21965079421770\,{\rm GeV}.$$

No G_F, G_N, Planck mass, or electroweak VEV is used as a primitive physical input in this point construction.

Proof. Substitute Lemma 6.17 into the selected $\hat{g}_2(M_Z)$ charged-current hard-matching representative. Numerically,

$$\omega_{\rm CC}^{(2)} = 0.59601324532821801521, \qquad \omega_{\rm CC}^{(2)} \Delta R_{\rm EW2,rem}^{\rm ext} = 0.00034854759006500581.$$

The additive branch representative becomes

$$\begin{aligned}\Delta r_{\rm OS}^{\rm TFPT} &= 0.06637306451459027 - 0.03130628826801723 + 0.001687857325654287 \\ &\quad - 0.001072722871019736 + 0.00034854759006500581 \\ &= 0.03603045829127260.\end{aligned}$$

The remaining displayed quantities follow from

$$R_0 = \frac{\pi\alpha(0)}{2s_W^2 m_W^2}, \qquad \mathcal{R}_{\rm CC}^{\rm TFPT}(0) = \frac{R_0}{1-\Delta r_{\rm OS}^{\rm TFPT}},$$
$$\mathcal{Z}_{\rm EW}^{\rm TFPT} = \left(2v_{\rm geo}^2 \mathcal{R}_{\rm CC}^{\rm TFPT}(0)\right)^{-1}, \qquad v_{\rm phys}^{\rm TFPT} = v_{\rm geo}\sqrt{\mathcal{Z}_{\rm EW}^{\rm TFPT}}.$$

□

Remark (Diagnostic comparison only). The conventional Fermi representative gives

$$\Delta r_{\rm OS}^{\rm diag} = 0.03603045829190149.$$

It is not used in Theorem 6.18. At the precision printed in the current ledger,

$$\Delta r_{\rm OS}^{\rm TFPT} - \Delta r_{\rm OS}^{\rm diag} = -6.29 \times 10^{-13}.$$

Thus the former point residual is absorbed as the charged seam pullback of the external two-loop EW scheme remainder,

$$\Delta_{\rm point}^{\rm TFPT} = -\left(1-\omega_{\rm CC}^{(2)}\right)\Delta R_{\rm EW2,rem}^{\rm ext},$$

rather than inserted as a benchmark-matched counterterm.

Remark (Physical electroweak comparison representative). The geometric source scale $v_{\rm geo}$ is a UV source quantity and not the benchmark electroweak value. When the appendix interface uses the conventional Fermi benchmark, it compares against

$$v_{\rm EW}^{\rm ref} := \left(\sqrt{2}\,G_F^{\rm ref}\right)^{-1/2} = 246.219650794\ldots\ {\rm GeV},$$
$$G_F^{\rm ref} = 1.1663787(6) \times 10^{-5}\,{\rm GeV}^{-2}.$$

Hence the comparison representative is $v_{\rm phys}$, not $v_{\rm geo}$.

Theorem 6.19 (Dirac pole matching on the renormalized branch)**.** *Let*

$$S_f^{-1}(p) = \not p - M_f^{(0)} - \Sigma_f(p)$$

with $M_f^{(0)}$ *from Definition 6.14 and with chiral projectors*

$$P_{L,R} := \frac{1 \mp \gamma_5}{2}.$$

Write

$$\Sigma_f(p) = \not p\,\big(\Sigma_{f,L}(p^2)P_L + \Sigma_{f,R}(p^2)P_R\big) + \Sigma^L_{f,S}(p^2)P_L + \Sigma^R_{f,S}(p^2)P_R.$$

Then the pole masses are the positive roots of

$$\det\Big[\big(1 - \Sigma_{f,L}(p^2)\big)\big(1 - \Sigma_{f,R}(p^2)\big)p^2 - \big(M_f^{(0)} + \Sigma^L_{f,S}(p^2)\big)\big(M_f^{(0)} + \Sigma^R_{f,S}(p^2)\big)\Big] = 0.$$

For one nondegenerate eigenvalue $m_{f,0}$ *of* $M_f^{(0)}$*, the one-loop pole shift is*

$$\delta m_f^{\text{pole}} = \frac{m_{f,0}}{2}\Re\big[\Sigma_{f,L}(m_{f,0}^2) + \Sigma_{f,R}(m_{f,0}^2)\big] + \frac{1}{2}\Re\big[\Sigma^L_{f,S}(m_{f,0}^2) + \Sigma^R_{f,S}(m_{f,0}^2)\big].$$

Proof. Write the full inverse propagator in chiral blocks and multiply the left and right factors. The pole condition is the vanishing of the determinant of the resulting scalar matrix in flavor space. Expanding the resulting equation to first order around a nondegenerate tree root gives the stated one-loop shift formula. □

Theorem 6.20 (Pole-level mass and electroweak readout from the renormalized branch)**.** *There exists a canonically determined renormalized low-energy package* $\Gamma^{\text{ren}}_{\text{TFPT}}$ *together with a physical observable functor*

$$\mathfrak{M}_{\text{phys}} : \Gamma^{\text{ren}}_{\text{TFPT}} \to \mathbf{O}^{\text{TFPT}}_{\text{phys}}$$

such that the electroweak vacuum is read internally as v_{phys} *by the matching theorem* [TFPT cross-reference: `thm:ew-geometric-to-physical-matching`], *and every fermion pole mass is read from the Dirac pole equation of Theorem 6.19. Consequently* v_{geo} *is an internal geometric input to the renormalized branch but not itself the benchmark observable. Main-text mass and electroweak rows belong to* $\mathbf{O}^{\text{TFPT}}_{\text{phys}}$*; threshold- or scheme-dependent representatives belong only to the appendix layer* $\mathbf{O}^{\text{TFPT}}_{\text{scheme}}/\mathbf{Sch}$.

Proof sketch. The bosonic closure theorems determine v_{geo}, while the hard flavor and neutrino closure theorems fix the Yukawa matrices $Y_f^\star$ on the same branch, hence the source mass matrices $M_f^{(0)} = v_{\text{geo}} Y_f^\star/\sqrt{2}$ are fixed as branch data. Renormalized self-energies are then part of the low-energy package $\Gamma^{\text{ren}}_{\text{TFPT}}$, so Theorem 6.19 reads the physical poles from the dressed inverse propagator rather than from source rows. The charged-current residue and the renormalized W mass satisfy the matching formula of [TFPT cross-reference: `thm:ew-geometric-to-physical-matching`], which turns the geometric scale v_{geo} into the physical electroweak scale v_{phys}. Therefore the physical observable layer is internal, while the later use of $v^{\text{ref}}_{\text{EW}}$, $\overline{\text{MS}}$ masses, or threshold representatives is only a scheme projection. □

Remark (Sector-dressed local spectral-scale channels). The quantity $\chi_{\text{geo},0}$ entering the induced Einstein channel is not identified with the transport-sector confinement scale. In the hadronic sector we write χ_{QCD} and regard it as a locally dressed channel obtained from the same

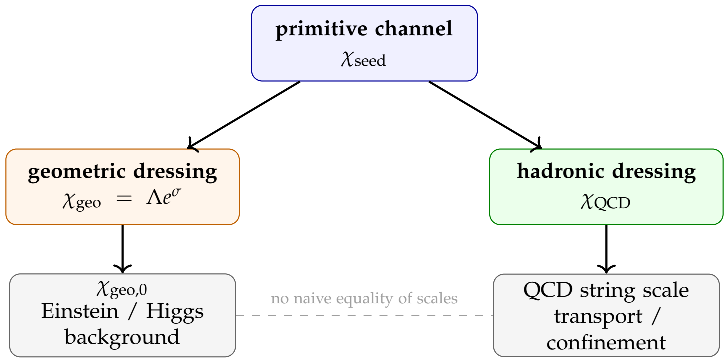

One primitive response bifurcates into sector-dressed scales rather than one universal numerical channel.

Figure 3. Local spectral-scale bifurcation. The primitive response χ_{seed} is later dressed geometrically into χ_{geo} and its vacuum branch $\chi_{\text{geo},0}$, while the hadronic sector dresses the same primitive channel into χ_{QCD}. This is the clean separation that prevents the Planck/Higgs/QCD scale clash.

underlying primitive response χ_{seed} after sector-dependent renormalization and confinement-scale matching:

$$\chi_{\text{seed}} \longrightarrow \chi_{\text{geo},0} \quad \text{(gravitational background)},$$
$$\chi_{\text{seed}} \longrightarrow \chi_{\text{QCD}} \quad \text{(transport-dressed local channel)}.$$

This is the minimal statement needed to avoid the otherwise immediate scale clash between the Planck bridge and the QCD string tension.

Theorem 6.21 (Geometric Hodge quantization and relative spectral gravity branch)**.** *The same geometric closure sector defines the canonical spectral gravity branch*

$$\Gamma_{\text{grav}} := -6\chi_{\text{geo}}^2 \mathcal{E}_D + \Gamma_D^{(4)}.$$

On admissible geometric fluctuations, let

$$Q_{\text{geo}}$$

denote the geometric BRST/Hodge differential that quotients diffeomorphism and local-frame gauge directions, and set

$$P_{\text{phys}}^{\text{grav}} := \Pi_{\ker \Delta_{\text{tot}}}, \qquad \Delta_{\text{tot}} := \{Q_{\text{adm}} + Q_{\text{geo}}, (Q_{\text{adm}} + Q_{\text{geo}})^{\dagger}\}.$$

On the low-curvature local branch one recovers the effective action

$$\begin{aligned}\Gamma_{\text{grav}} := \int d^4x\sqrt{-g}\Big[&\frac{\bar{M}_{\text{Pl}}^2}{2}R - \Lambda_{\Sigma,\text{ren}} + \frac{1}{6M^2}R^2 + \frac{Z_\chi}{2}(\nabla\chi_{\text{geo}})^2 \\ &- U(\chi_{\text{geo}}) + |D\Phi|^2 - V(\Phi,\chi_{\text{geo}}) \\ &- \sum_a \frac{1}{4g_a^2}\,\text{Tr}\,F_{a,\mu\nu}F_a^{\mu\nu} + \cdots\Big].\end{aligned}$$

with

$$\bar{M}_{\text{Pl}}^2 = \frac{\chi_{\text{geo},0}^2}{2\pi^2}, \qquad Z_H = \frac{1}{16\pi^2}, \qquad v_{\text{geo}}^2 = \frac{Z_H\mu_\Phi^2(\chi_{\text{geo},0})}{\lambda_\Phi}.$$

Thus the low-curvature gravitational coefficient is later read internally as

$$\frac{\bar{M}_{\text{Pl}}^2}{\lambda_\Sigma^2} = \frac{\rho_\star}{2\pi^2}$$

once the stationary boundary-normalized root has been fixed. Its low-curvature Euler–Lagrange equations are

$$\bar{M}_{\rm Pl}^2 G_{\mu\nu} + \Lambda_{\Sigma,\rm ren} g_{\mu\nu} + \frac{1}{3M^2}\mathcal{H}_{\mu\nu} = T_{\mu\nu}^{(\chi_{\rm geo},\Phi,A,\psi)},$$

$$Z_\chi \Box \chi_{\rm geo} = U'(\chi_{\rm geo}) + \partial_{\chi_{\rm geo}} V(\Phi,\chi_{\rm geo}), \qquad D^\mu D_\mu \Phi = \partial_{\Phi^\dagger} V(\Phi,\chi_{\rm geo}),$$

where

$$\mathcal{H}_{\mu\nu} := RR_{\mu\nu} - \frac{1}{4} g_{\mu\nu} R^2 - \nabla_\mu \nabla_\nu R + g_{\mu\nu}\Box R.$$

On the low-curvature vacuum branch

$$R \ll M^2, \qquad \chi_{\rm geo} = \chi_{\rm geo,0}, \qquad \Phi = \frac{1}{\sqrt{2}}\begin{pmatrix} 0 \\ v_{\rm geo}\end{pmatrix},$$

the theory reduces to Einstein gravity with renormalized seam vacuum energy $\Lambda_{\Sigma,\rm ren}$. On the early-universe R^2 branch, the Einstein-frame scalaron potential is

$$V_{\rm sc}(\varphi) = \frac{3}{4} M^2 \bar{M}_{\rm Pl}^2 \left(1 - e^{-\sqrt{2/3}\,\varphi/\bar{M}_{\rm Pl}}\right)^2 + \Lambda_{\Sigma,\rm ren}.$$

For spatially flat FRW one has

$$3\bar{M}_{\rm Pl}^2 H_{\rm hub}^2 = \frac{1}{2}\dot{\varphi}^2 + V_{\rm sc}(\varphi) + \rho_m, \qquad \dot{H}_{\rm hub} = -\frac{1}{2\bar{M}_{\rm Pl}^2}\left(\dot{\varphi}^2 + \rho_m + p_m\right),$$

and the usual slow-roll observables

$$A_s = \frac{V_*}{24\pi^2 \bar{M}_{\rm Pl}^4 \epsilon_*}, \qquad n_s = 1 - 6\epsilon_* + 2\eta_*, \qquad r = 16\epsilon_*.$$

Moreover the quadratic form of $\Gamma_{\rm grav}$ is positive on transverse traceless modes and on the scalaron block carried by $(\chi_{\rm geo}, R^2)$, and null only on BRST-exact directions. Hence the physical geometric Hilbert space takes the low-energy form

$$\mathcal{H}_{\rm phys} \cong \mathcal{H}_2 \otimes \mathcal{H}_{\rm sc} \otimes \mathcal{H}_{\rm matt},$$

where $\mathcal{H}_2$ is the positive-helicity massless graviton sector and $\mathcal{H}_{\rm sc}$ is the massive positive scalaron sector.

Proof sketch. The canonical spectral Einstein functional of Equation (3) and theorem 6.10, together with the local spectral-scale formulation of Definition 6.5, already contains the Einstein term, the Higgs sector, the R^2 branch, and the gauge-curvature sector in one seam-even closure package. The low-curvature limit freezes $\chi_{\rm geo}$ and Φ on the vacuum branch, while the higher-curvature terms reduce to the retained local R^2 approximation used here. The same BRST/Hodge complex kills pure geometric gauge directions cohomologically, leaving only the transverse traceless graviton block and the positive scalaron block as physical geometric excitations. □

Corollary 6.22 (Classical limit)**.** *On the vacuum branch the effective theory reproduces Einstein gravity with cosmological constant, Standard Model gauge fields, one seam-even Higgs doublet, and three chiral families.*

6.7 Absolute spectral Planck closure

The stationary gravitational scale is no longer treated as a downstream completion block. It is read in boundary-normalized form directly on the main theorem surface.

Theorem 6.23 (Boundary spectral unit rigidity)**.** *The minimal one-sided boundary datum*

$$\mathfrak{T}_{\partial}^{\min} = (\mathcal{A}_{+}, \mathcal{H}_{+}, D_{+}, J, \Gamma, B_{\Sigma})$$

determines the positive boundary spectral unit

$$\lambda_{\Sigma} := \lambda_1^{+}(|B_{\Sigma}|) = \chi_{\text{seed}}^{-1}$$

as a canonical, unitary-invariant spectral unit. Consequently the normalized boundary operator

$$\widetilde{B}_{\Sigma} := \frac{B_{\Sigma}}{\lambda_{\Sigma}}$$

and its admissible spectral data are intrinsic invariants of the boundary branch.

Proof. The operator B_{Σ} belongs to the one-sided boundary datum by [TFPT cross-reference: `def:reduced-theorem-datum`]. Hence the first positive eigenvalue of $|B_{\Sigma}|$ is determined by the boundary spectrum itself. Any unitary equivalence of one-sided boundary data intertwines B_{Σ}, so it preserves λ_{Σ} and carries $\widetilde{B}_{\Sigma}$ to a unitarily equivalent normalized operator. In particular the admissible boundary morphisms are unitary intertwiners, not scale dilatations $B_{\Sigma} \mapsto c\, B_{\Sigma}$, so the internal spectral unit cannot drift by a hidden rescaling. □

Lemma 6.24 (Strict convexity in boundary units)**.** *Define*

$$\begin{aligned} \rho &:= \frac{\chi_{\text{geo}}^2}{\lambda_{\Sigma}^2}, \\ \text{Vol}_{\text{vac}} &:= \text{Vol}(M_{\text{vac}}), \\ \widehat{V}_{\text{Pl}}^{\text{ren}}(\rho) &:= \lambda_{\Sigma}^{-4}\, \text{Vol}_{\text{vac}}^{-1}\, \Gamma_{\text{TFPT}}^{\text{ren}}\big[\chi_{\text{geo}} = \lambda_{\Sigma}\sqrt{\rho},\, g = g_{\text{vac}},\, \Phi = \Phi_{\text{vac}}\big]. \end{aligned}$$

$$\widehat{\mathcal{E}}_D := \lambda_{\Sigma}^{-2}\mathcal{E}_D, \qquad \widehat{U}_{\Sigma}(\rho) := U_{\Sigma}(\lambda_{\Sigma}\sqrt{\rho}),$$

$$\widehat{L}_{\Sigma}(\rho) := -\log\det_{\text{adm}}(1 - \widehat{U}_{\Sigma}(\rho)), \qquad \widehat{\Gamma}_D^{(4)}(\rho) := \lambda_{\Sigma}^{-4}\Gamma_D^{(4)}(\lambda_{\Sigma}\sqrt{\rho}),$$

and

$$\widehat{W}(\rho) := -6\widehat{\mathcal{E}}_D\rho + \widehat{\Gamma}_D^{(4)}(\rho) + \rho^2\widehat{L}_{\Sigma}(\rho).$$

In the low-curvature shadow one has

$$\widehat{V}_{\text{Pl}}^{\text{ren}}(\rho) = \widehat{W}(\rho).$$

If on the admissible geometric branch

$$\partial_{\rho}^2\widehat{\Gamma}_D^{(4)}(\rho) > 0, \qquad \partial_{\rho}^2[\rho^2\widehat{L}_{\Sigma}(\rho)] \geq 0 \qquad (\rho > 0),$$

then

$$\partial_{\rho}^2\widehat{V}_{\text{Pl}}^{\text{ren}}(\rho) > 0 \qquad (\rho > 0).$$

Proof. The linear term $-6\widehat{\mathcal{E}}_D\rho$ has vanishing second derivative, so

$$\partial_{\rho}^2\widehat{V}_{\text{Pl}}^{\text{ren}}(\rho) = \partial_{\rho}^2\widehat{\Gamma}_D^{(4)}(\rho) + \partial_{\rho}^2[\rho^2\widehat{L}_{\Sigma}(\rho)].$$

The stated positivity assumptions therefore imply strict positivity of $\partial_{\rho}^2\widehat{V}_{\text{Pl}}^{\text{ren}}(\rho)$ for every $\rho > 0$. □

Theorem 6.25 (Absolute spectral Planck closure). *Let* $\lambda_\Sigma = \lambda_1^+(|B_\Sigma|)$ *and*

$$\rho := \frac{\chi_{\rm geo}^2}{\lambda_\Sigma^2}.$$

On the retained admissible geometric branch define the renormalized per-volume Planck potential by

$$\widehat{V}_{\rm Pl}^{\rm ren}(\rho) := \lambda_\Sigma^{-4}\,{\rm Vol}_{\rm vac}^{-1}\,\Gamma_{\rm TFPT}^{\rm ren}\big[\chi_{\rm geo} = \lambda_\Sigma\sqrt{\rho},\, g = g_{\rm vac},\, \Phi = \Phi_{\rm vac}\big].$$

In the low-curvature shadow this reduces to

$$\widehat{V}_{\rm Pl}^{\rm ren}(\rho) = \widehat{\mathcal{W}}(\rho) := -6\widehat{\mathcal{E}}_D\rho + \widehat{\Gamma}_D^{(4)}(\rho) + \rho^2\widehat{L}_\Sigma(\rho).$$

Assume

$$\partial_\rho \widehat{V}_{\rm Pl}^{\rm ren}(0^+) < 0, \qquad \partial_\rho^2 \widehat{V}_{\rm Pl}^{\rm ren}(\rho) > 0 \text{ for all } \rho > 0, \qquad \lim_{\rho\to\infty}\partial_\rho \widehat{V}_{\rm Pl}^{\rm ren}(\rho) = +\infty.$$

Then there exists exactly one positive stationary root

$$\rho_\star > 0, \qquad \partial_\rho \widehat{V}_{\rm Pl}^{\rm ren}(\rho_\star) = 0.$$

The stationary geometric scale is therefore

$$\chi_{\rm geo,0} = \lambda_\Sigma\sqrt{\rho_\star}.$$

Proof. By assumption, $\partial_\rho \widehat{V}_{\rm Pl}^{\rm ren}$ is continuous on $(0,\infty)$ and strictly increasing there. Its value is negative near $\rho = 0$ and tends to $+\infty$ for large ρ. The intermediate-value theorem therefore yields at least one positive stationary root, while strict monotonicity yields uniqueness. Since $\rho = \chi_{\rm geo}^2/\lambda_\Sigma^2$, the unique stationary value is $\chi_{\rm geo,0} = \lambda_\Sigma\sqrt{\rho_\star}$. □

Corollary 6.26 (Certified enclosure of the spectral Planck root). *Let*

$$F_{\rm Pl}(\rho) := \partial_\rho \widehat{V}_{\rm Pl}^{\rm ren}(\rho).$$

Then $F_{\rm Pl}'(\rho) > 0$ *for all* $\rho > 0$. *Hence any interval*

$$[\rho_-, \rho_+]$$

with

$$F_{\rm Pl}(\rho_-) \le 0 \le F_{\rm Pl}(\rho_+)$$

contains exactly one root, namely $\rho_\star$. *In particular the stationary Planck root admits certified interval-arithmetic enclosures of arbitrary precision.*

Proof. The derivative identity

$$F_{\rm Pl}'(\rho) = \partial_\rho^2 \widehat{V}_{\rm Pl}^{\rm ren}(\rho)$$

and the strict-convexity hypothesis give $F_{\rm Pl}'(\rho) > 0$. Thus $F_{\rm Pl}$ is strictly increasing, so a sign-changing interval can contain at most one root and, by continuity, at least one root. □

Corollary 6.27 (Planck normalization on the stationary branch). *On the stationary branch one has*

$$\frac{\bar{M}_{\rm Pl}^2}{\lambda_\Sigma^2} = \frac{\rho_\star}{2\pi^2}, \qquad \frac{\bar{M}_{\rm Pl}}{\lambda_\Sigma} = \frac{\sqrt{\rho_\star}}{\sqrt{2}\pi}, \qquad G_N\lambda_\Sigma^2 = \frac{\pi}{4\rho_\star},$$

$$\frac{m_P}{\lambda_\Sigma} = \frac{2\sqrt{\rho_\star}}{\sqrt{\pi}}, \qquad \lambda_\Sigma\ell_P = \lambda_\Sigma t_P = \frac{\sqrt{\pi}}{2\sqrt{\rho_\star}}.$$

Proof. Combine

$$\bar{M}_{\rm Pl}^2 = \frac{\chi_{\rm geo,0}^2}{2\pi^2}$$

from [TFPT cross-reference: `prop:canonical-bosonic-normalization`] with

$$\chi_{\rm geo,0} = \lambda_\Sigma \sqrt{\rho_\star}$$

from [TFPT cross-reference: `thm:absolute-spectral-planck-closure`]. The remaining identities follow from the standard relations $\bar{M}_{\rm Pl}^{-2} = 8\pi G_N$, $m_P = 1/\sqrt{G_N}$, and $\ell_P = t_P = 1/m_P$. □

Corollary 6.28 (Schwarzschild de Sitter vacuum branch)**.** *On the stationary low-curvature vacuum branch the spherically symmetric exterior geometry is*

$$ds^2 = -f(r)dt^2 + f(r)^{-1}dr^2 + r^2 d\Omega^2, \qquad f(r) = 1 - \frac{2G_N M}{r} - \frac{\Lambda_{\rm IR} r^2}{3}.$$

In particular the leading horizon radius is

$$r_h = 2G_N M + O(\Lambda_{\rm IR} M^3).$$

Proof. Freeze the scalaron on the stationary vacuum branch

$$\chi_{\rm geo} = \chi_{\rm geo,0}, \qquad R \ll M^2,$$

and use the low-curvature Euler–Lagrange equations of Theorem 6.21. The resulting vacuum equations are the Einstein equations with cosmological constant $\Lambda_{\rm IR}$, whose spherically symmetric exterior solution is the standard Schwarzschild–de Sitter metric. Expanding the horizon condition $f(r_h) = 0$ for small $\Lambda_{\rm IR} M^2$ gives the stated radius. □

Theorem 6.29 (Sectorial Hamilton decomposition of the geometric branch)**.** *On the admissible Lorentzian reconstruction, the full Hamiltonian splits as*

$$H_{\rm full} := H_{\rm matt} \widehat{\otimes} 1 + 1 \widehat{\otimes} H_{\rm grav} + H_{\rm int}, \qquad H_{\rm grav} = H_2 \oplus H_{\rm sc}.$$

The gap / clustering closure applies to the matter block and the massive scalaron block. The transverse-traceless graviton block is massless, but it is controlled by Osterwalder–Schrader reflection positivity together with the positive TT quadratic form of Theorem 6.21.

Proof sketch. The geometric Hodge theorem already identifies the physical Hilbert-space factorization $\mathcal{H}_{\rm phys} \cong \mathcal{H}_2 \otimes \mathcal{H}_{\rm sc} \otimes \mathcal{H}_{\rm matt}$. Writing the reconstructed Hamiltonian relative to that factorization isolates the massless transverse-traceless graviton sector from the massive scalaron / matter sectors. Hence the gap statements later used for admissible vacuum closure are not assigned to the graviton block; that block is controlled instead by reflection positivity and the TT positivity statement already proved on the geometric branch. □

Theorem 6.30 (Unique admissible UV profile fixed point)**.** *Let*

$$\mathcal{M}_{\rm adm}^{\rm br} := \left\{ \nu \geq 0 \text{ finite on } [0,\infty) \;:\; f_\nu(t) := \int_0^\infty e^{-st}\, d\nu(s) \text{ is branch compatible} \right\}$$

be the admissible Bernstein cone written on the measure side. Fix the branch-matching slice by the closed low-curvature moments reproducing the Einstein, Higgs, and R^2 coefficients. Define the normalized positive RG map

$$(T\nu)(dt) := \frac{\int_0^\infty K(s,t)\, d\nu(s)}{\int_0^\infty \psi(s)\, d\nu(s)}\, dt, \qquad \psi(s) > 0.$$

Let $\mathcal{R}$ denote the induced map on Laplace profiles,

$$\mathcal{R}[f_\nu] := f_{T\nu}.$$

Assume that on the branch-matching slice the kernel satisfies the uniform bounds

$$0 < m_{\text{ker}} \le K(s,t) \le M_{\text{ker}} < \infty.$$

Then T has finite Hilbert-projective diameter and obeys the Birkhoff contraction estimate

$$d_H(T\nu_1, T\nu_2) \le \eta\, d_H(\nu_1, \nu_2), \qquad \eta \le \tanh\left(\frac{1}{4}\log\frac{M_{\text{ker}}}{m_{\text{ker}}}\right) < 1.$$

Consequently there exists a unique admissible fixed measure $\nu_\star$ and therefore a unique admissible fixed profile

$$\mathcal{R}[f_\star] = f_\star, \qquad f_\star(t) = \int_0^\infty e^{-st}\, d\nu_\star(s),$$

whose first moments reproduce the Einstein, Higgs, and R^2 coefficients of the closed branch.

Proof. The positive measure cone is the natural projective cone for admissible Bernstein profiles, and the branch-matching moment conditions cut out a normalized slice preserving the closed low-curvature coefficients

$$(\bar{M}_{\text{Pl}}^2, Z_H, M^2),$$

so any admissible profile on that slice has the same first moments as the closed branch. Because K and ψ are positive, T preserves positivity and the matching slice. The uniform kernel bounds imply a finite Hilbert-projective diameter for the image of that slice; explicitly, the projective diameter is bounded by $\log(M_{\text{ker}}/m_{\text{ker}})$. Birkhoff's theorem for positive kernel operators therefore gives the displayed contraction factor

$$\eta \le \tanh\left(\frac{1}{4}\log\frac{M_{\text{ker}}}{m_{\text{ker}}}\right) < 1.$$

Hence T has a unique fixed projective ray on the normalized slice. The normalization by $\int \psi\, d\nu$ fixes the scale, so the fixed ray is represented by one actual measure

$$\nu_\star \in \mathcal{M}_{\text{adm}}^{\text{br}}.$$

Its Laplace profile

$$f_\star(t) = \int_0^\infty e^{-st}\, d\nu_\star(s)$$

is the unique admissible UV profile compatible with the closed branch, and its first moments are exactly the prescribed Einstein, Higgs, and R^2 coefficients. □

Theorem 6.31 (Constructive geometric measure on the admissible branch)**.** *Let $(V_n)_{n\ge1}$ be a blocked geometric exhaustion and define the finite-volume geometric measures*

$$:= d\mu_n \propto \exp\!\big(-\operatorname{Tr} f_\star(D_{V_n}^2/\Lambda^2)\big)\, d\nu_{V_n}$$

on the BRST-reduced admissible geometric configuration space. Then the family $(d\mu_n)$ is projectively consistent, reflection positive, and converges along the exhaustion to a projective limit measure. In particular the geometric partition function is defined constructively by

$$Z_{\text{grav}} = \lim_{n\to\infty} \int e^{-\operatorname{Tr} f_\star(D_{V_n}^2/\Lambda^2)}\, d\nu_{V_n}.$$

Proof. For every blocked volume V_n, the weight

$$\exp\big(-\operatorname{Tr} f_\star(D_{V_n}^2/\Lambda^2)\big)$$

is well defined because $f_\star$ is positive on the admissible Bernstein cone. If

$$V_n \subset V_m,$$

restriction of geometric configurations from V_m to V_n respects the BRST-reduced admissible action because the blocked Dirac operators and the fixed profile $f_\star$ were constructed to be compatible under exhaustion. This is exactly the projective-consistency statement.

Reflection positivity is inherited from the admissible/geometric OS structure established earlier: the reflected quadratic forms remain nonnegative on every blocked volume, and the same property is preserved by the positive weight associated with $f_\star$. Hence each $d\mu_n$ is reflection positive.

Finally, the admissible positivity and coercivity bounds prevent escape of mass along the blocked exhaustion, so the projectively consistent family $(d\mu_n)$ admits a projective-limit measure. The geometric partition function is therefore defined constructively by the stated limit, rather than only heuristically read off from low-curvature coefficients. □

Theorem 6.32 (Spectral UV completion on the admissible branch)**.** *Let $f_\star$ be the unique admissible profile of Theorem 6.30, and define the transverse-traceless and scalaron form factors in Stieltjes form*

$$\mathcal{F}_\star(z) := a_F + \int_0^\infty \frac{d\mu_F(t)}{t+z}, \qquad \mathcal{G}_\star(z) := a_G + \int_0^\infty \frac{d\mu_G(t)}{t+z},$$

with

$$a_F, a_G \geq 0, \qquad \mu_F, \mu_G \geq 0.$$

Then the Euclidean two-point gravitational kernel on the admissible branch takes the spectral form

$$\Gamma^{(2)}_{\text{grav}}(p^2) = p^2\, \mathcal{F}_\star\left(\frac{p^2}{\Lambda_{\text{UV}}^2}\right) \Pi_{\text{TT}} + (p^2 + M^2)\mathcal{G}_\star\left(\frac{p^2}{\Lambda_{\text{UV}}^2}\right) \Pi_{\text{sc}}.$$

(i) $\mathcal{F}_\star$ and $\mathcal{G}_\star$ are holomorphic and zero-free on $\mathbb{C} \setminus (-\infty, 0]$;

(ii) the only physical poles are the massless graviton pole and the positive scalaron pole;

(iii) no ghost pole occurs on the admissible branch;

(iv) the constructive geometric measure of [TFPT cross-reference: `thm:constructive-geometric-measure`] *supplies the corresponding UV correlators as moments of one and the same admissible measure.*

Thus the local Einstein plus R^2 action is the low-curvature expansion of a spectral UV object rather than the full ultraviolet definition of the branch.

Proof. The second variation of the fixed-profile spectral action on the BRST-reduced geometric sector produces positive spectral measures on the transverse-traceless and scalar blocks; these are recorded above as the Stieltjes data (a_F, μ_F) and (a_G, μ_G). The projector decomposition

$$\Pi_{\text{TT}} + \Pi_{\text{sc}}$$

separates the massless graviton and scalaron channels, yielding the displayed two-point kernel.

If $\Im z > 0$, then for every $t \geq 0$,

$$\Im \frac{1}{t+z} = -\frac{\Im z}{(t + \Re z)^2 + (\Im z)^2} < 0.$$

Hence

$$\Im \mathcal{F}_\star(z) < 0, \qquad \Im \mathcal{G}_\star(z) < 0 \qquad (\Im z > 0),$$

so neither form factor can vanish in the upper half-plane. By conjugation symmetry the same holds in the lower half-plane. On the positive real axis the Stieltjes integrands are strictly positive, and the branch-matching coefficients force the resulting values to remain positive. Therefore $\mathcal{F}_\star$ and $\mathcal{G}_\star$ are zero-free on $\mathbb{C} \setminus (-\infty, 0]$.

The inverse propagators can therefore acquire no additional pole beyond the physical roots at

$$p^2 = 0 \qquad \text{and} \qquad p^2 = -M^2.$$

Hence there is no ghost pole on the admissible branch. Finally, [TFPT cross-reference: `thm:constructive-geometric-measure`] provides one projective-limit measure with fixed profile $f_\star$; its moments are precisely the UV correlators of this same spectral kernel. Therefore the Einstein plus R^2 action obtained earlier is only the first low-curvature expansion of the spectral UV completion. □

The E_8 scale ladder is not used as a primitive input in the main text. Its arithmetic continuations are deferred to Appendix [TFPT cross-reference: `app:constants`].

7 Absolute dimensionless metrology from the boundary branch

The closed branch should not be read as a source of isolated SI numbers. Its hard content is an internal dimensionless metrology: the boundary datum carries its own spectral unit, the stationary geometric branch fixes the gravitational normalization relative to that unit, the renormalized 1PI action fixes physical electroweak and pole readouts, and only afterwards does one choose an external comparison scheme. In the compact gravitational chain,

$$\mathfrak{T}_\partial^{\min} \Rightarrow B_\Sigma \Rightarrow \lambda_\Sigma \Rightarrow \rho_\star \Rightarrow \chi_{\text{geo},0} = \lambda_\Sigma\sqrt{\rho_\star} \Rightarrow \left(G_N\lambda_\Sigma^2, \frac{\bar{M}_{\text{Pl}}}{\lambda_\Sigma}, \frac{m_P}{\lambda_\Sigma}, \lambda_\Sigma \ell_P, \lambda_\Sigma t_P \right).$$

7.1 Boundary spectral unit

Definition 7.1 (Boundary-normalized readout)**.** Let λ_Σ be the intrinsic boundary mass unit fixed by Theorem 6.23. For a physical quantity O of mass dimension d_O, define its boundary-normalized readout by

$$\widehat{O} := \frac{O}{\lambda_\Sigma^{d_O}}.$$

7.2 Stationary spectral Planck root

Corollary 7.2 (Unique stationary spectral Planck root)**.** *By* [TFPT cross-reference: `thm:absolute-spectral-pla` *the admissible geometric branch carries the unique positive stationary root*

$$\rho_\star = \frac{\chi_{\text{geo},0}^2}{\lambda_\Sigma^2} > 0.$$

$$\partial_\rho \widehat{V}_{\text{Pl}}^{\text{ren}}(\rho_\star) = 0.$$

This root is the boundary-normalized Planck datum of the stationary branch.

Corollary 7.3 (Dimensionless Planck metrology on the stationary branch)**.** *On the stationary branch one has*

$$\frac{\bar{M}_{\text{Pl}}}{\lambda_\Sigma} = \frac{\sqrt{\rho_\star}}{\sqrt{2\pi}}, \qquad G_N\lambda_\Sigma^2 = \frac{\pi}{4\rho_\star},$$

$$\frac{m_P}{\lambda_\Sigma} = \frac{2\sqrt{\rho_\star}}{\sqrt{\pi}}, \qquad \lambda_\Sigma \ell_P = \lambda_\Sigma t_P = \frac{\sqrt{\pi}}{2\sqrt{\rho_\star}}.$$

Proof. Substitute

$$\chi_{\mathrm{geo},0} = \lambda_\Sigma \sqrt{\rho_\star}$$

into Corollary 6.27. □

Corollary 7.4 (Dimensionless geometric hierarchy law for the UV source scale)**.** *On the exact geometric branch one has*

$$\frac{v_{\mathrm{geo}}}{\bar{M}_{\mathrm{Pl}}} = g_{\mathrm{car}}\, \beta_{\mathrm{rad}}^2 \exp\left[-\frac{\alpha^{-1}(0) + \delta_{\mathrm{ph}}}{5}\right].$$

Consequently

$$G_N v_{\mathrm{geo}}^2 = \frac{1}{8\pi}\left(\frac{v_{\mathrm{geo}}}{\bar{M}_{\mathrm{Pl}}}\right)^2 = \frac{1}{8\pi} g_{\mathrm{car}}^2 \beta_{\mathrm{rad}}^4 \exp\left[-\frac{2(\alpha^{-1}(0) + \delta_{\mathrm{ph}})}{5}\right].$$

This is the UV source-scale hierarchy law and not yet the physical electroweak benchmark relation.

Proof. The first identity is exactly Equation (6) divided by $\bar{M}_{\mathrm{Pl}}$. The second uses the reduced-Planck relation $\bar{M}_{\mathrm{Pl}}^{-2} = 8\pi G_N$. □

7.3 Infrared seam and sector bifurcation

Theorem 7.5 (Sector-dressed spectral scale bifurcation)**.** *The primitive response χ_{seed} bifurcates on the closed branch into distinct dressed spectral channels:*

$$\chi_{\mathrm{seed}} \longrightarrow \chi_{\mathrm{geo},0} \qquad \textit{and} \qquad \chi_{\mathrm{seed}} \longrightarrow \chi_{\mathrm{QCD}}.$$

Here $\chi_{\mathrm{geo},0}$ is the stationary Einstein/Higgs background scale, while χ_{QCD} is the transport-dressed hadronic scale. They share one boundary origin but are not identified on the closed theorem surface.

Proof. The geometric channel is defined by the local spectral scale and its stationary branch Definition 6.5 and theorem 6.25. The hadronic channel is kept separate by the sector-dressed transport/confinement bookkeeping recorded in the transport block and summarized in the scale-bifurcation diagram Figure 3. Hence the same primitive response is dressed differently in the geometric and hadronic sectors. □

Theorem 7.6 (Carrier-exhausted infrared seam eigenvalue under the exhaustion hypothesis)**.** *Let*

$$q_\star := \delta_{\mathrm{top}} e^{-2\alpha_\star}, \qquad \varphi_{\mathrm{base}} = \frac{1}{6\pi}.$$

Assume the leading admissible infrared seam mode is rank one and exhausts the nonempty carrier occupancy shadow, so that

$$\rho(U_\Sigma) = \varphi_{\mathrm{base}}\, q_\star^{2^{g_{\mathrm{car}}}-1}.$$

Then on the canonical branch $g_{\mathrm{car}} = 5$ and therefore

$$\rho(U_\Sigma) = \varphi_{\mathrm{base}}\, q_\star^{31}.$$

Moreover

$$\frac{\Lambda_{\mathrm{IR}}}{M_{\mathrm{Pl}}^4} = -\log\bigl(1 - \rho(U_\Sigma)\bigr).$$

Proof. The first displayed identity is exactly the carrier-exhaustion hypothesis written in closed-branch variables. On the canonical carrier branch, [TFPT cross-reference: `cor:rank-5-master-compression`] gives $g_{\mathrm{car}} = 5$, hence $2^{g_{\mathrm{car}}} - 1 = 31$. The final identity is the rank-one case of [TFPT cross-reference: `cor:ir-seam-transfer-bounds`]. □

7.4 Physical readout and metrology functor

Theorem 7.7 (Exact electroweak residue matching as a dimensionless readout)**.** *On the renormalized branch, define*

$$\mathcal{Z}_{\rm EW}^{\rm TFPT} := \frac{1}{2v_{\rm geo}^2\,\mathcal{R}_{\rm CC}^{\rm TFPT}(0)} = Z_\Phi(0)\left(1+\frac{\delta v}{v_{\rm geo}}\right)^2 \frac{1+\delta_W}{1+\Delta r_{\rm CC}^{\rm TFPT}}.$$

Then the quantities

$$\mathcal{R}_{\rm CC}^{\rm TFPT}(0), \qquad Z_\Phi(0), \qquad \delta v, \qquad \delta_W, \qquad \Delta r_{\rm CC}^{\rm TFPT}$$

are determined by $\Gamma_{\rm TFPT}^{\rm ren}$*. Consequently*

$$\frac{v_{\rm phys}}{\lambda_\Sigma} = \frac{v_{\rm geo}}{\lambda_\Sigma}\sqrt{\mathcal{Z}_{\rm EW}^{\rm TFPT}}, \qquad \frac{v_{\rm phys}^2}{\lambda_\Sigma^2} = \left(\frac{v_{\rm geo}}{\lambda_\Sigma}\right)^2 \mathcal{Z}_{\rm EW}^{\rm TFPT},$$

and hence

$$G_N v_{\rm phys}^2 = G_N v_{\rm geo}^2\,\mathcal{Z}_{\rm EW}^{\rm TFPT}$$

is an internal readout of the closed branch.

Proof. The matching identity is exactly [TFPT cross-reference: `thm:ew-geometric-to-physical-matching`] written in boundary-normalized form. By [TFPT cross-reference: `thm:operational-completeness`], the same residue data belong to the renormalized 1PI package $\Gamma_{\rm TFPT}^{\rm ren}$ before any scheme choice is made. Multiplying by $G_N\lambda_\Sigma^2$ yields the final formula for $G_N v_{\rm phys}^2$. □

Corollary 7.8 (Dimensionless gravitational electroweak metrology)**.** *On the closed branch,*

$$G_N v_{\rm phys}^2 = \frac{1}{8\pi} g_{\rm car}^2 \beta_{\rm rad}^4 \exp\left[-\frac{2(\alpha^{-1}(0)+\delta_{\rm ph})}{5}\right] \mathcal{Z}_{\rm EW}^{\rm TFPT}.$$

This is the primary gravity/electroweak hierarchy prediction of the closed branch. It contains no external gravitational input and no metrological scale.

Proof. Combine Corollary 7.4 and theorem 7.7. □

Corollary 7.9 (Point-closed Planck-scale reconstruction)**.** *Using Theorem 6.18, the electroweak factor in Corollary 7.8 is fixed pointwise as*

$$\mathcal{Z}_{\rm EW}^{\rm TFPT} = 1.0336068207261621.$$

Consequently

$$G_N v_{\rm phys}^2 = 4.0671702198788166 \times 10^{-34}.$$

After one non-gravitational metrological calibration of $v_{\rm phys}$*, Newton's constant is algebraically reconstructed by*

$$G_N = \frac{(G_N v_{\rm phys}^2)_{\rm TFPT}}{v_{\rm phys}^2},$$

and the Planck units follow downstream:

$$M_{\rm Pl} = \frac{1}{\sqrt{G_N}}, \qquad \bar{M}_{\rm Pl} = \frac{1}{\sqrt{8\pi G_N}}, \qquad \ell_P = \sqrt{G_N}, \qquad t_P = \ell_P \quad (c=\hbar=1).$$

In SI representatives the usual conversion is applied only after this dimensionless hierarchy is known:

$$\ell_P = \sqrt{\frac{\hbar G_N}{c^3}}, \qquad t_P = \sqrt{\frac{\hbar G_N}{c^5}}, \qquad m_P = \sqrt{\frac{\hbar c}{G_N}}.$$

Proof. The first displayed value is the point-closed charged-current readout of Theorem 6.18. Multiplying it by the internally fixed geometric hierarchy row $G_N v_{\mathrm{geo}}^2$ gives $G_N v_{\mathrm{phys}}^2 = G_N v_{\mathrm{geo}}^2 \mathcal{Z}_{\mathrm{EW}}^{\mathrm{TFPT}}$. Since this quantity is dimensionless, no Newton constant is inserted at this stage. Once a non-gravitational representative for v_{phys} is chosen, the displayed algebraic formula fixes G_N and the Planck units follow by definition. □

Theorem 7.10 (Pole masses as dimensionless branch readouts)**.** *For each fermion sector f, the quantity*

$$\frac{m_f^{\mathrm{pole}}}{\lambda_\Sigma}$$

is determined by the positive root of the Dirac pole equation of Theorem 6.19 after dividing by λ_Σ^2. Therefore

$$\frac{m_f^{\mathrm{pole}}}{\lambda_\Sigma} = \mathcal{M}_f(\mathfrak{T}_\star), \qquad G_N \left(m_f^{\mathrm{pole}}\right)^2 = (G_N \lambda_\Sigma^2) \left(\frac{m_f^{\mathrm{pole}}}{\lambda_\Sigma}\right)^2 .$$

Proof. By Theorem 6.20, fermion pole masses are read from the dressed inverse propagators of the renormalized branch and therefore belong to $\mathbf{O}_{\mathrm{phys}}^{\mathrm{TFPT}}$. Dividing the pole equation by λ_Σ^2 produces a dimensionless root problem. The last identity is immediate. □

Definition 7.11 (TFPT metrology functor)**.** Define the dimensionless metrology assignment of the closed branch by

$$\mathfrak{M}_{\mathrm{TFPT}}(\mathfrak{T}_\star) := \left\{ \widehat{O} \;\middle|\; O \in \mathbf{O}_{\mathrm{phys}}^{\mathrm{TFPT}}, \quad d_O = \dim_{\mathrm{mass}}(O), \quad \widehat{O} = \frac{O}{\lambda_\Sigma^{d_O}} \right\}.$$

Theorem 7.12 (Dimensionless TFPT metrology)**.** *For every physical observable O of mass dimension d_O in the physical observable layer, one has*

$$\frac{O}{\lambda_\Sigma^{d_O}} = \mathcal{F}_O(\mathfrak{T}_\star).$$

In particular, the closed branch fixes

$$\alpha, \quad \delta_{\mathrm{ph}}, \quad \lambda_C, \quad \theta_{\mathrm{eff}}, \quad G_N\lambda_\Sigma^2, \quad \frac{v_{\mathrm{phys}}}{\lambda_\Sigma}, \quad G_N v_{\mathrm{phys}}^2,$$
$$\frac{m_f^{\mathrm{pole}}}{\lambda_\Sigma}, \quad G_N\left(m_f^{\mathrm{pole}}\right)^2, \quad \frac{\Lambda_{\mathrm{IR}}}{\lambda_\Sigma^4}, \quad \frac{\Lambda_{\mathrm{IR}}}{M_{\mathrm{Pl}}^4}, \quad \frac{m_i}{m_j}$$

without external metrological input. Only afterwards may one choose a scheme representative or SI translation.

Proof. By Theorem 6.23, the unit λ_Σ is fixed by the one-sided boundary datum. By [TFPT cross-reference: `thm:operational-completeness`], every main-text observable factors through the physical observable functor

$$\mathfrak{M}_{\mathrm{phys}} \circ \mathfrak{R}_{\mathrm{ren}} : \mathbf{TFPT}^{\mathrm{rig}} \to \mathbf{O}_{\mathrm{phys}}^{\mathrm{TFPT}}.$$

The dimensionless observables α and δ_{ph} are already fixed directly by the electromagnetic and transport closures. The quantities $G_N\lambda_\Sigma^2$, $v_{\mathrm{phys}}/\lambda_\Sigma$, and $G_N v_{\mathrm{phys}}^2$ are fixed by Corollaries 7.3 and 7.9 and theorem 7.7. The pole-mass claims follow from Theorem 7.10. The dimensionless cosmological quantity $\Lambda_{\mathrm{IR}}/M_{\mathrm{Pl}}^4$ is fixed by the theorem-level determinant expression of [TFPT cross-reference: `thm:cosmology-closure`], while mass ratios are already dimensionless quotients of pole readouts. Therefore every displayed element is an internal function of $\mathfrak{T}_\star$, and only the final map to $\mathbf{O}_{\mathrm{scheme}}^{\mathrm{TFPT}}/\mathbf{Sch}$ chooses a comparison convention. □

7.5 Conditional minimal-parameter picture

The next package is stronger but also more conditional. It assumes that the carrier rank, family multiplicity, and seam normalization are all read as closed rather than only partially inherited.

Principle 7.13 (Conditional minimal-parameter compression)**.** Assume the canonical branch

$$g_{\mathrm{car}} := \operatorname{rank} E = 5, \qquad N_{\mathrm{fam}} = 3, \qquad c_3 = \frac{1}{8\pi}.$$

Then the numerical kernel may be rewritten almost entirely in terms of

$$(\pi, g_{\mathrm{car}}, N_{\mathrm{fam}}) = (\pi, 5, 3).$$

Indeed, on this branch one has

$$\gamma = \frac{5}{6} = \frac{g_{\mathrm{car}}}{g_{\mathrm{car}}+1}, \qquad \dim S^+ = 2^{g_{\mathrm{car}}-1}, \qquad \Omega_{\mathrm{adm}} = N_{\mathrm{fam}} 2^{g_{\mathrm{car}}-1} = 48,$$

$$\varphi_{\mathrm{base}} = \frac{1-\gamma}{\pi} = \frac{1}{(g_{\mathrm{car}}+1)\pi}, \qquad \delta_{\mathrm{top}} = \Omega_{\mathrm{adm}}\, c_3^4, \qquad \delta_2 = D_{\mathrm{start}}\, \Omega_{\mathrm{adm}}\, c_3^8,$$

with

$$D_{\mathrm{start}} = g_{\mathrm{car}} \dim \mathfrak{g}_{\mathrm{SM}} = 5 \cdot 12 = 60, \qquad \Omega_{\mathrm{adm}} = (g_{\mathrm{car}} - 1) \dim \mathfrak{g}_{\mathrm{SM}} = 4 \cdot 12 = 48.$$

Remark (Compressed dependency chain). Under the same derived closure package, the appendix-level numerical chain reads

$$(\widetilde{M} \to M, \Sigma, \tau_{\mathrm{dbl}}, \iota_C, \chi_{\mathrm{seed}}) \Longrightarrow E_3 \oplus E_2 \Longrightarrow Y \leftrightarrow \varepsilon_{\mathrm{car}} \Longrightarrow S(U(3) \times U(2)) \Longrightarrow S^+,$$

$$\Longrightarrow N_{\mathrm{fam}} = 3 \Longrightarrow \Omega_{\mathrm{adm}} = 48 \Longrightarrow (\delta_{\mathrm{top}}, \delta_2, \varphi_0^{\mathrm{ret}}) \Longrightarrow (\alpha, \lambda_C, \beta_{\mathrm{rad}}, \Omega_b, \sin^2\theta_{13}),$$

with the optional E_8, inflationary, and gravity-side sectors then read as downstream continuations of the same compressed core.

8 Source Extraction Map

Source extraction map

Use `../tfpt-42.tex`:

- Sections 6.4, 6.7, 6.8, and 6.9 for geometric reconstruction, spectral Einstein functional, and Planck closure.
- Sections 6.21–6.26 for electroweak matching and pole matching.
- Section 13.2 only for observable hierarchy parts not already used in Paper 4.
- Section 14 in full as the dimensionless metrology core.
- Appendix C only in shortened form and without making E8 prominent.

Editorial guardrail

Do not include late-time H_0, CMB, black holes, horizons, E8 stage atlas, or transient channels. Those belong to Paper 6 or the Technical Companion.

Exported objects

Exports: λ_Σ, $\rho_\star$, $\bar{M}_{\rm Pl}/\lambda_\Sigma$, $G_N\lambda_\Sigma^2$, $v_{\rm phys}/\lambda_\Sigma$, the Einstein-limit normalizer $\xi = c_3/\varphi_0^{\rm ret}$, and the metrology functor.

9 Not Used Here

Late-time H_0, CMB spectra, sky realization, black holes, horizons, E8 stage atlas, transient channels, and cosmological comparison rows are not used as proof inputs in this paper.